Article

RETRACTED: Chitosan-Based Microparticles Enhance Ellagic Acid's Colon Targeting and Proapoptotic Activity

Nabil A. Alhakamy [1,2,3], **Osama A. A. Ahmed** [1], **Mallesh Kurakula** [4], **Giuseppe Caruso** [5],
Filippo Caraci [5,6], **Hani Z. Asfour** [7], **Anas Alfarsi** [1], **Basma G. Eid** [8], **Amir I. Mohamed** [9],
Nabil K. Alruwaili [10], **Wesam H. Abdulaal** [11], **Usama A. Fahmy** [1], **Hani A. Alhadrami** [12,13],
Basmah M. Eldakhakhny [14] **and Ashraf B. Abdel-Naim** [8,*]

1 Department of Pharmaceutics, Faculty of Pharmacy, King Abdulaziz University, Jeddah 21589, Saudi Arabia; nalhakamy@kau.edu.sa (N.A.A.); oaahmed@kau.edu.sa (O.A.A.A.); mr_alfarsi8@hotmail.com (A.A.); uahmedkauedu.sa@kau.edu.sa (U.A.F.)

2 Advanced Drug Delivery Research Group, Faculty of Pharmacy, King Abdulaziz University, Jeddah 21589, Saudi Arabia

3 Center of Excellence for Drug Research and Pharmaceutical Industries, King Abdulaziz University, Jeddah 21589, Saudi Arabia

4 Department of Biomedical Engineering, University of Memphis, Memphis, TN 38152, USA; mkrakula@memphis.edu

5 Oasi Research Institute—IRCCS, Via Conte Ruggero, 73, 94018 Troina, Italy; forgiuseppecaruso@gmail.com (G.C.); fcaraci@unict.it (F.C.)

6 Department of Drug Sciences, University of Catania, 95125 Catania, Italy

7 Department of Medical Microbiology and Parasitology, Faculty of Medicine, King Abdulaziz University, Jeddah 21589, Saudi Arabia; hasfour@kau.edu.sa

8 Department of Pharmacology and Toxicology, Faculty of Pharmacy, King Abdulaziz University, Jeddah 21589, Saudi Arabia; beid@kau.edu.sa

9 Department of Pharmaceutics and Industrial Pharmacy, Military Medical Academy, Cairo 11757, Egypt; miroami@gmail.com

10 Department of Pharmaceutics, Faculty of Pharmacy, Jouf University, Skaka P.O. Box 2014, Saudi Arabia; nabilalruwaili@gmail.com

11 Department of Biochemistry, Cancer Metabolism and Epigenetic Unit, Faculty of Science, King Abdulaziz University, Jeddah 21589, Saudi Arabia; whabdulaal@kau.edu.sa

12 Department of Medical Laboratory Technology, Faculty of Applied Medical Sciences, King Abdulaziz University, P.O. Box 80402, Jeddah 21589, Saudi Arabia; hanialhadrami@kau.edu.sa

13 Special Infectious Agent Unit (Biosafety Level 3), King Fahd Medical Research Centre, P.O. Box 80402, Jeddah 21589, Saudi Arabia

14 Department of Clinical Biochemistry, Faculty of Medicine, King Abdulaziz University, Jeddah 21589, Saudi Arabia; beldakhakhny@kau.edu.sa

* Correspondence: abnaim@yahoo.com; Tel.: +966-55-6814781

check for updates

Abstract: This study aimed at improving the targeting and cytotoxic effect of ellagic acid (EA) on colon cancer cells. EA was encapsulated in chitosan (CHIT) polymers then coated by eudragit S100 (ES100) microparticles. The release of EA double-coated microparticles (MPs) was tested at simulative pH values. Maximum release was observed at 24 h and pH 7.4. The cytotoxicity of EA MPs on HCT 116 colon cancer cells was synergistically improved as compared with raw EA. Cell-cycle analysis by flow cytometry suggested enhanced G2-M phase colon cancer cell accumulation. In addition, a significantly higher cell fraction was observed in the pre-G phase, which highlighted the enhancement of the proapoptotic activity of EA formulated in the double-coat mixture. Annexin-V staining was used for substantiation of the observed cell-death-inducing activity. Cell fractions were significantly increased in early, late, and total cell death. This was backed by high elevation in cellular content of caspase 3. Effectiveness of the

double-coated EA to target colonic tissues was confirmed using real-time iohexol dye X-ray radiography. In conclusion, CHIT loaded with EA and coated with ES100 formula exhibits improved colon targeting as well as enhanced cytotoxic and proapoptotic activity against HCT 116 colon cancer when compared with the administration of raw EA.

Keywords: chitosan; ellagic acid; drug release; muco-adhesion; colon targeting

1. Introduction

Colon or bowel cancer, also known as colorectal cancer (CRC), is the third deadliest type of cancer around the world. About two-thirds of recorded cases appeared in developed countries [1–3]. The main risk factors for this type of cancer are old age, inflammatory intestinal conditions, low-fiber diet, high-fat diet, and sedentary lifestyle. Genetic disorders can also cause CRC; however, less than 5% of CRC are due to inherited genetic disorders [4–7]. Common treatment options include surgery, chemotherapy, radiation, and targeted therapy. Most cases may require more than one method of treatment [8,9]. However, most of these treatments generate undesired side effects, toxicity, and patient discomfort. Further, these adverse effects may be reduced or eliminated via targeted drug delivery. This provides many benefits compared with conventional drug delivery medicines such as increased drug efficiency and stability as well as reduced adverse effects and toxicity. Because of their safety and effectiveness, natural products are gaining more attention toward their utilization in cancer chemotherapy [7]. In this regard, polyphenols are promising and have the ability to modulate cell signaling cascades to induce cancer cell death. Ellagic acid (EA) is a polyphenol that is present naturally in fruits and nuts. Several in vivo and in vitro studies highlighted the anticancer properties of EA against different cancer types, including colon, bladder, breast, and lung cancers [10–14]. Also, its antioxidative and anti-inflammatory properties are well-documented [15]. The antioncogenic effects of EA against colon cancer cells in leptin-enriched microenvironments have been demonstrated [16]. EA has also been reported to control genomic stability and prevent cancerous mutations [10,17,18]. Nevertheless, EA's low-water solubility (0.8 mg/mL) and inferior bioavailability (0.2% oral bioavailability) have greatly limited its therapeutic value [19]. Poor absorption, hepatic first-pass effect, and rapid elimination are attributed to low EA oral bioavailability [11,20–23]. However, the use of targeted drug delivery techniques can help to overcome these obstacles. This can be achieved by the use of the biocompatible polymers chitosan (CHIT) as a carrier for an effective and efficient delivery of EA [24,25]. CHIT is a polycationic polysaccharide derived from deacetylation of chitin [26,27]. The use of CHIT as a natural carrier of controlled release drugs was previously reported [28,29]. This is due to its improved cost effectiveness, biocompatibility, bioavailability, biodegradability, and reduced toxicity. CHIT glycosidic bonds are hydrolyzed at the colon and fully digested by enzymes in colonic bacteria [25,30]. The use of CHIT as a drug carrier grants increased residence time in the gastrointestinal (GI) tract through mucoadhesion as well as improved cellular permeability [31].

Glutaraldehyde has been used as a cross-linking agent for protein reactions [32,33]. The mechanism of glutaraldehyde cross-linking with proteins is pH-dependent. In addition, in the case of CHIT, the degree of amino groups protonation also determines the solubility of this polysaccharide in water [34]. At pH 5.6, the anions of glutaraldehyde were formed. It is assumed that the cross-linking by glutaraldehyde involves two carbonyl groups of glutaraldehyde [35].

Since CHIT is degradable in an acidic environment, an enteric coating is usually used to guard against gastric acidity and ensure colon targeting [25,30,36,37]. Functional polymers play an important role when it comes to controlled drug release formulations. Poly(meth)acrylates, which are known as EUDRAGIT® polymers, are commonly employed and offer several advantages in various formulations [38–40]. Eudragit enteric coating polymers contain free carboxylic acid groups [41]. Eudragit S100 (ES100) is insoluble in the stomach because of being unionized in acidic conditions.

At high pH media, the acid groups become ionized and the film coating dissolves, releasing the drug at that point. In this way, manipulating the free carboxylic groups will increase the ability of the drug to be released at the exact pH in the correct target environment. ES100 is an ionic polymer that contains carboxylic acid groups (pKa 6) in its backbone. The dissolution threshold of ES 100 is pH 7 (colonic pH), where the majority of the carboxylic groups are ionized [41]. In this study, an enteric coating of CHIT-loaded EA with ES100 in the form of microparticles (MPs) was investigated, aimed at enhanced colon targeting efficiency and improved EA cytotoxicity against HCT 116 cells.

2. Materials and Methods

2.1. Materials

Ellagic acid (EA), CHIT from shrimp shells (≥75% deacetylated), McCoy's 5a medium, trypsin-0.02% EDTA, PBS, Dulbecco's modified Eagle medium (DMEM), and the fetal bovine serum (FBS) were from Sigma Aldrich (St. Louis, MO, USA). Eudragit® S100 (ES100) was a kind gift from Evonik Industries AG (Essen, Germany). Corning Transwell® polycarbonate membrane 12-well and 96-well plates were obtained from Corning Co., Ltd., (New York, USA). Cell-counting kit 8 (CCK-8) was obtained from Boster Biological Technology Co., Ltd., (Pleasanton, CA, USA). Chemicals used were of analytical or HPLC grade.

2.2. Preparation of CHIT-Coated MPs

CHIT MPs were prepared according to the two step-operation procedure developed by Thakral et al. [30]. Briefly, CHIT was dissolved in a 0.5% acetic acid aqueous solution to form a CHIT solution at room temperature with stirring, and the solution was adjusted to pH 5.5 using 0.01 mol/L NaOH. EA was dispersed in the CHIT solution (1.5% *w/v*) in a drug-to-polymer ratio of 1:5 EA:CHIT ratio. The dispersion was passed through a 24-gauge needle into liquid paraffin, which contains 2% span 80 stirred at 2000 rpm by a mechanical stirrer. After that, glutaraldehyde (10 mL, 25% *v/v*) was added to the dispersion. Then, 1 and 2 h after glutaraldehyde addition, a further 5 mL of glutaraldehyde solution was added at each time point (1 and 2 h). After that, the dispersion was stirred for an additional 1 h. Liquid paraffin was then decanted, and EA-CHIT MPs were retrieved, washed using petroleum ether, and air dried for 4 h. After that, the prepared MPs were then lyophilized (Martin Christ Gefriertrocknungsanlagen GmbH, Osterode am Harz, Germany) at −45 °C and pressure of 0.07 mbar for 24 h.

For encapsulation (coating) of core EA-CHIT MPs with ES100, the prepared EA-CHIT MPs were dispersed in ES100 solution (10% *w/v*) in acetone-ethanol (2:1). The dispersion was then dropped into mechanically stirred liquid paraffin containing 2% span 80. Stirring continued for 4 h to evaporate the acetone-ethanol organic solvent. Petroleum ether was used to wash the filtered EA-CHIT-coated ES100 MPs, which were air-dried for 4 h and then vacuum oven-dried for 24 h at room temperature.

2.3. Characterization of EA-CHIT-ES100 MPs

2.3.1. Scanning Electron Microscopy

Double-face tape was used for holding the metal stubs in place in which the samples were placed for analysis. Soldering of the tape to the aluminum stubs was carried out beforehand, and a vacuum was used to apply a gold coating. To facilitate proper visualization of the surface morphology of the MPs formula, a scanning electron microscope (JSM-7610F; JEOL, Tokyo, Japan) was employed.

2.3.2. Encapsulation Efficiency and Loading Capacity

A high-performance liquid chromatography (HPLC) protocol was utilized. A sample of the prepared formula was dispersed in ethanol and sonicated using a Vibra-Cell ultrasonic processor (VCX 750, Sonics & Materials, Inc., Newtown, CT, USA) to dissolve entrapped EA and was then filtered

through a 0.22 μm filter. Equations (1) and (2) were applied to calculate the encapsulation efficiency (EE %) and loading capacity (LC %) of EA.

$$EE\,\% = \left(\frac{Amount\ of\ drug\ in\ the\ formula}{Amount\ of\ drug\ initially\ added}\right) \times 100 \tag{1}$$

$$LC\,\% = \left(\frac{Drug\ mass\ in\ MPs}{Mass\ of\ MPs}\right) \times 100 \tag{2}$$

2.3.3. EA In Vitro Release from EA-CHIT-ES100 MPs

Coated microspheres were accurately weighed to correspond to 2 mg of EA and were placed in a 0.1 M KCl/HCl buffer (250 mL, pH 1.2) and magnetically stirred at 50 rpm at 37 °C for 2 h (0.5, 1, 1.5 and 2 h time intervals). After 2 h in the buffer (pH 1.2), the solution was substituted with 250 mL of 0.1 M potassium dihydrogen orthophosphate buffer pH 4.5 for 2 h (2.5, 3, 3.5, and 4 h time intervals) and then substituted with 250 mL of 0.1 M phosphate buffer pH 7.4 (4.5, 5, 5.5, 6, and 24 h time intervals). Centrifugation, filtration (0.45 μm membrane filter), and analysis of EA content was carried out for the withdrawn samples. Triplicates of the tests were carried out. HPLC was utilized for EA concentration analysis of the aliquots, as previously described.

2.4. Cell Culture

HCT 116 and EA.hy926 cells were purchased from Vacsera (Giza, Egypt). Cells were kept in McCoy's 5a medium. EA.hy926 cells were maintained in Dulbecco's modified Eagle's medium. Heat-inactivated fetal bovine serum (10%), penicillin (100 units/mL), and streptomycin (100 μg/mL) were present in the culture medium. Cells were kept in a subconfluent state, in 5% CO2 (*v/v*) humidified atmosphere, at 37 °C.

2.5. Cytotoxicity Assessment

For cytotoxicity assessment of the prepared EA MPs, EA, and PLAIN MPs (plain formula) against the HCT 116 cells and sulforhodamine B (SRB) was employed; further, 96-well plates (1000–2000 cells/well) were used for cell seeding [42]. Cells were treated for 72 h with serial concentrations of the prepared formulae. Trichloroacetic acid (TCA) (10%) was then added for 1 h at 4 °C for cell fixation. Distilled water was used to wash the cells several times. This was followed by staining with a 0.4% SRB solution. Plates were maintained for 10 min at ambient temperature in the dark. Consequently, cells were washed using 1% glacial acetic acid. Tris-HCl was used to dissolve the SRB-stained cells after overnight drying of the plates. A monochromator SpectraMax® M3 plate reader (Molecular Devices, Sunnyvale, CA, USA) was employed for color intensity (OD) determination at 540 nm. OD values were used to calculate IC_{50} values.

The impact of the combining EA in the CHIT-ES100 double-coat on the cytotoxicity of EA was assessed using the isobologram equation [43] for interaction index (I) determination as follows:

$$I = \frac{d1}{Dy,1} + \frac{d2}{Dy,2} \tag{3}$$

where *d*1, *d*2 are concentrations of drug 1 and drug 2 in mixture, giving an effect *y*, while *Dy*,1 and *Dy*,2 are the concentrations of drug 1 and drug 2 giving the same effect *y* if taken alone. If "*I*" was less than 1, it was considered a synergistic combination; however, *I* = 1 or *I* > 1, which suggests an additive or antagonistic effect, respectively.

2.6. Analysis of Cell Cycle Progression

Six-well culture plates were used to seed about 3×10^5 cells/well. Over 24 h, the cells were placed in treatment-free media (control incubations), 1.6 μM EA MPS and equivalent concentrations of plain MPs and pure EA. CycleTEST™ PLUS DNA Reagent Kit (Becton Dickinson Immunocytometry

Systems, San Jose, CA, USA) was employed for analysis of the cell cycle. The DI (DNA Index) of the tested preparations was determined in reference to cells with a predetermined content of DNA. Staining was carried out using propidium iodide. Finally, CELLQUEST software (Becton Dickinson Immunocytometry Systems, San Jose, CA, USA) was used to study distribution of the cell cycle.

2.7. Annexin-V Assay

The dual-staining technique was performed to assess apoptosis as previously published [44]. HCT 116 cells were incubated with PLAIN MPs, pure EA, and EA-MPs with reference to 1.6 μM EA. in a six-well plate with a cell density of 1×10^5 cells per well. A control sample with untreated cells was also included in the study. Staining was carried out using a commercially available kit (BD Bioscience, CA, USA), catalog number 556547). The kit contained a 10X annexin V binding buffer, FITC annexin V, and propidium iodide staining solution. After incubation for 24 h, the cells were obtained after centrifugation. The cells were then re-suspended in 500 μL of 1X binding buffer. The cells were kept in the dark for 5 min at room temperature in 5 μL each of annexin V-FITC V and propidium iodide staining solution. The cell analyzer BD FACS CaliburTM (BD Bioscience, Franklin Lakes, NJ, USA) was used to carry out the analyses. Multicycle software (Phoenix Flow Systems, San Diego, CA, USA) was used for data analysis.

2.8. Assay of Caspase-3 Enzyme

Cells were incubated under the same conditions as in the cell-cycle analysis for 24 h. A commercial kit (USCN Life Science Inc., China) was used to quantify caspase 3 after lysis of the cells and extraction.

2.9. Realtime X-Ray Radiography of the Contrast Medium Iohexol Formulated in CHIT-Coated ES100 in Rabbits

Handling of rabbits was approved by the Ethical Committee of Faculty of Pharmacy, Cairo University, Egypt. Rabbits were maintained under the following conditions: 12 h alternate light and dark cycle, relative humidity 45%, and room temperature. Optimum X-ray radiographic conditions were established. Animals were kept on standard food pellets and free access to water. Overnight fasted male New Zealand rabbits, weighing 2–2.2 kg were used. Animals separated into two groups (*n* = 6). The first group served as a control in which each rabbit was given a single oral plain capsule containing 100 mg of 48.5% *w/w* iohexol. Animals in the second group were administered capsules containing 48.5% *w/w* iohexol in CHIT for the prepared CHIT-ES 100 MPs (100 mg). Capsules were inserted behind the tongue to prevent them from being destroyed. A dose of iohexol was chosen based on a preliminary experiment. Animals were physically kept in rabbit restrainers. Targeting efficiency of the CHIT-coated ES100 MPs was determined by assessing the contrast generated by iohexol. Radiography was performed at 0.5 and 6 h using a villa X-ray medical system (Buccinasco MI, Italy).

2.10. Statistical Analysis

IBM SPSS statistics software, version 25 (SPSS Inc., Chicago, IL, USA), was used for statistical analysis. Means were compared by Analysis of Variance (ANOVA) followed by Tukey as a post hoc test. Data are given as Mean ± SD. $p < 0.05$ was deemed significant.

3. Results

3.1. Characterization of the EA-CHIT-ES100 MPs

In the present study, EA was formulated in CHIT MPs. The prepared MPs were then coated with ES100 to form colon-targeted MPs. Figure 1 shows an SEM image of MPs for both EA-CHIT (Figure 1A) and EA-CHIT coated with ES 100. The ES 100-coated MPs showed average particle size (200 ± 40 μm), with a smooth surface that demonstrated the entrapment of EA-CHIT-MPs in the ES100 MPs matrix (Figure 1B–D).
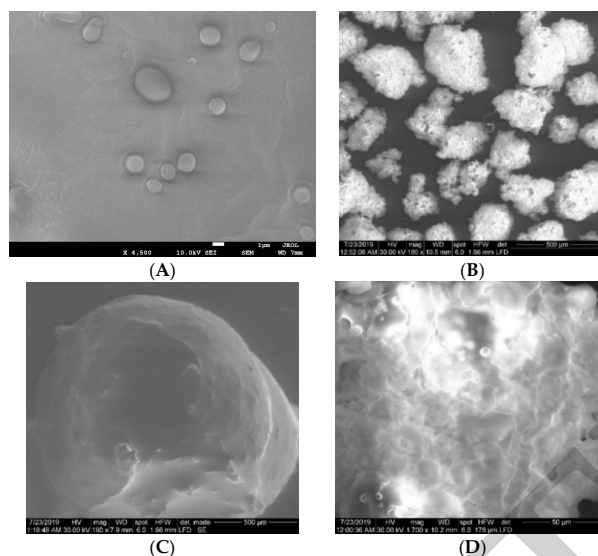
Figure 1. SEM images of microparticles (MPs) of chitosan loaded with ellagic acid (EA-CHIT) (**A**) and, additionally, coated with eudragit S100 (EA-CHIT-ES) at various magnifications: 180 X (**B**) 800 X (**C**) and 3000 X (**D**) showing EA-CHIT MPs entrapped within the ES100 coat.

The EA-MPs exhibited encapsulation efficiency (EE%) and loading capacity (LC%) amounting to 84.16 ± 3.91% and 10.52 ± 0.88%, respectively. The MPs characterization was further carried out by examining EA release. The percentage of EA released from the prepared MPs at different pH values (1.2, 4.5, and 7.2) compared with the raw EA is shown in Figure 2. At pH 1.2 and 4.5, no more than 8% of EA content released. At pH 7.2, the amount of EA released within the first 2 h reached about 55%. After 24 h at pH 7.2, EA-MPs demonstrated release of most EA content.

Figure 2. Release profile of EA MPs at different pH values (1.2, 4.5, and 7.4).

3.2. In Vitro Cytotoxicity

The IC_{50} values from the EA-CHIT-MPs against the HCT 116 cells show increased cytotoxicity, as shown in Figure 3A. PLAIN EA MPs showed IC50 value of 49.5 ± 4.2 μM, raw EA 11.70 ± 1.27 μM, and EA MPs 3.2 ± 0.31 μM. The interaction index was found to 0.85, indicating a synergistic interaction between EA and the formulated CHIT-ES100 double coat. Further, cytotoxicity of the same preparations was examined in the noncancerous cells EA.hu926 (Figure 3B). Plain MPs, raw EA, and EA MPs exhibited IC50 values of 86.9 ± 11.3, 50.52 ± 4.2 and 41.7 ± 3.7 μM, respectively. All values were referenced to positive control incubations containing staurosporine (STU).
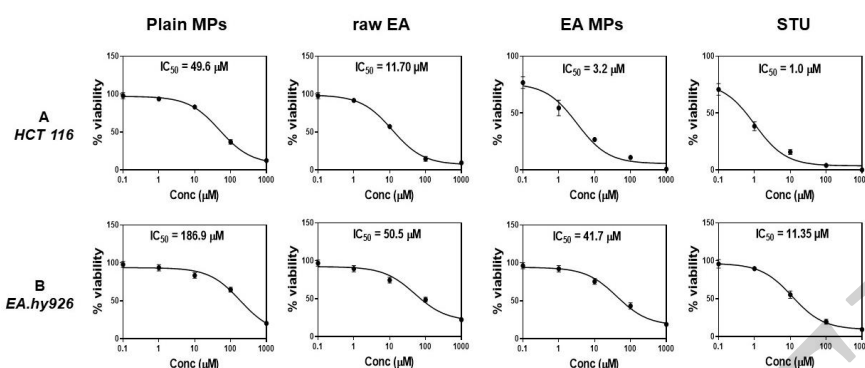
Figure 3. IC_{50} of plain MPs, raw EA, and the EA MPs in (**A**) the HCT 116 cells and (**B**) EA.hy926 cells.

3.3. Analysis of Progression of the Cell Cycle

HCT 116 cells, which were not treated (control), had quick growth properties, with $49.62 \pm 3.82\%$ in the G0/G1 phase, $36.15 \pm 2.1\%$ in the S phase, $14.14 \pm 1.2\%$ in the G2-M phase, and $2.07 \pm 0.05\%$ in the pre-G1 phase (Figure 4A). Proliferation of the HCT 116 cells was slower after incubation with EA, plain MPs, and EA-MPs, as indicated by accumulation of cells in the G2-M and pre-G1 phases (Figure 4B–D). Fractions of cellular population in the pre-G phase for incubations containing EA, Plain MPs, or EA-MPs were $16.26 \pm 0.9\%$, $16.51 \pm 0.7\%$, and $24.36 \pm 1.02\%$ of the control incubations, respectively. Graphical presentations of alterations in the cell-cycle phases after different treatments are shown in Figure 4E,F.
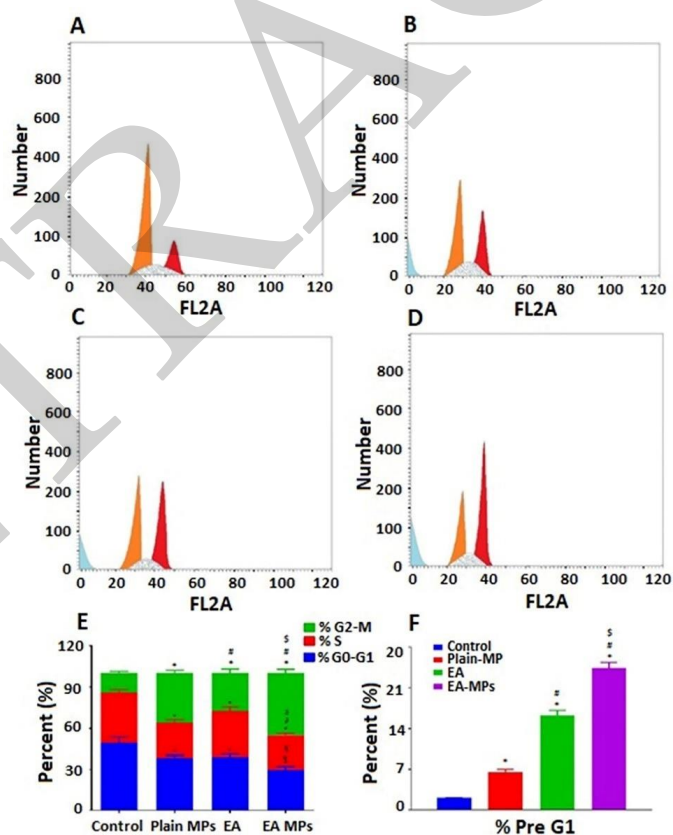

Figure 4. Impact of the EA MPs on the cell-cycle phases. (**A**) Control, (**B**) plain MPs, (**C**) raw EA, (**D**) EA MPs, (**E**) graphical presentation of each phase, and (**F**) graphical presentation of pre-G1 phase. * Significantly different from corresponding control at $p < 0.05$; # significantly different from plain MP at $p < 0.05$; $ significantly different from EA at $p < 0.05$.

3.4. Apoptosis Assay of Annexin V–FITC and Cellular Content of Caspase 3

To further substantiate the observed apoptotic effects, the percentage of cells with positive annexin-V staining was determined in the control, plain MPS, EA, and EA-MPs incubations (Figure 5A–D). There was a marked increase in early, late, and total cell death after incubation with EA MPs relative to the others. A graphical representation of the types of cell death is shown in Figure 5E.
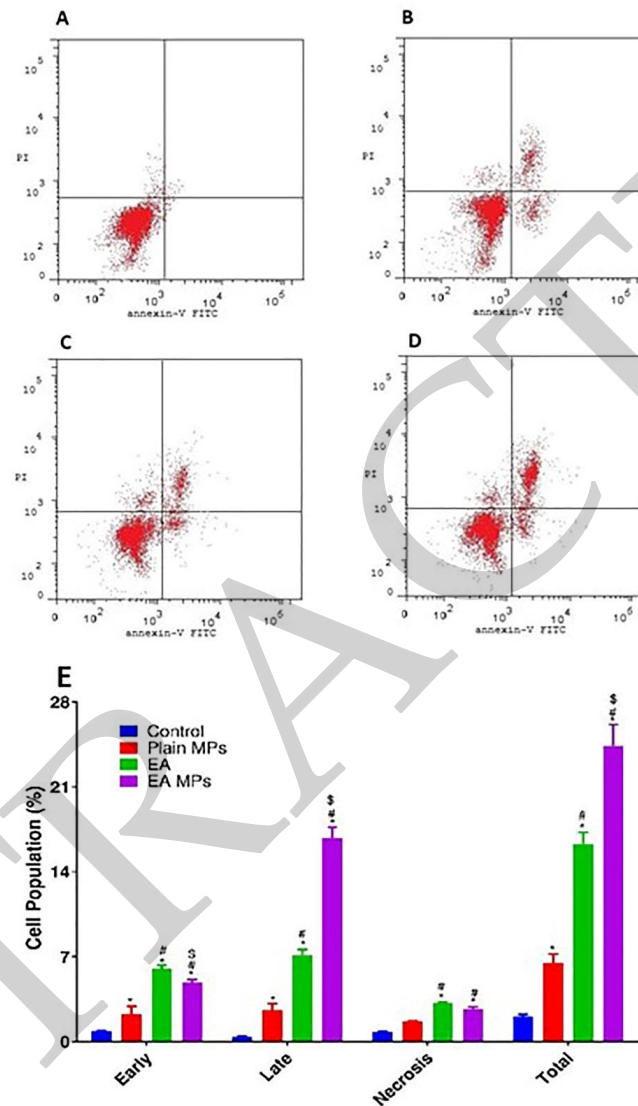

Figure 5. Impact of the EA MPs on the annexin-V fluorescein isothiocyanate (FITC) positive-staining HTC 116 cells. (**A**) Control, (**B**) plain MPs, (**C**) raw EA, (**D**) EA MPs, and (**E**) graphical presentation of early and late apoptotic, necrotic, and total cell death. * Significantly different from corresponding control at $p < 0.05$. # significantly different from plain MP at $p < 0.05$; $ significantly different from EA at $p < 0.05$.

Caspase 3 content was used for confirmation of the apoptotic effects caused by EA, EA MPs. Cells exposed to EA–MPs had a greater caspase 3 concentration (399.5 ± 17.7 pg/mg protein) when compared with the control (45.39 ± 4.12 pg/mL), raw EA (248.5 ± 18.27 pg/mg protein), and plain MPs (212.6 ± 13.7 pg/mg protein) incubations (Figure 6).
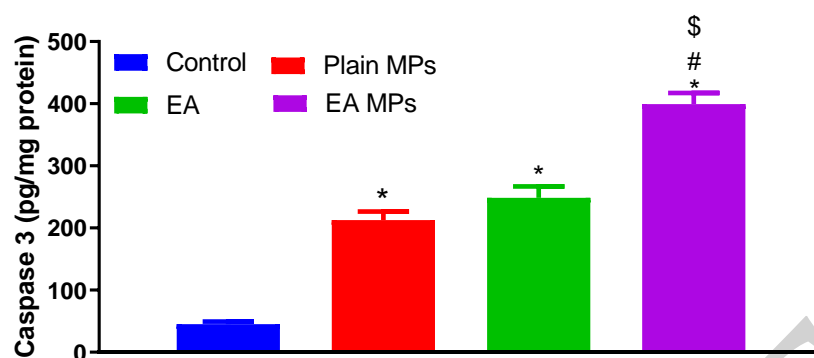
Figure 6. Effect of EA formulated in CHIT-ES100 double-coat on caspase 3 content in HCT 116 colon cancer cells. * Significantly different from control at $p < 0.05$; # significantly different from plain MPs at $p < 0.05$; $ significantly different EA at $p < 0.05$.

3.5. Realtime X-ray Radiography of Iohexol

Radio assessment of iohexol entrapped in CHIT ES100 indicated ability of the double-coated MPs to retain the dye in colonic tissues at 6 h after oral administration (Figure 7A). On the other hand, radiographic opacities were detected only at $\frac{1}{2}$ h when administering iohexol pure (control, no MPs) in size-2 hard gelatin capsules and was completely undetected in the whole Gastrointestinal tract (GIT) at 6 h (Figure 7B).
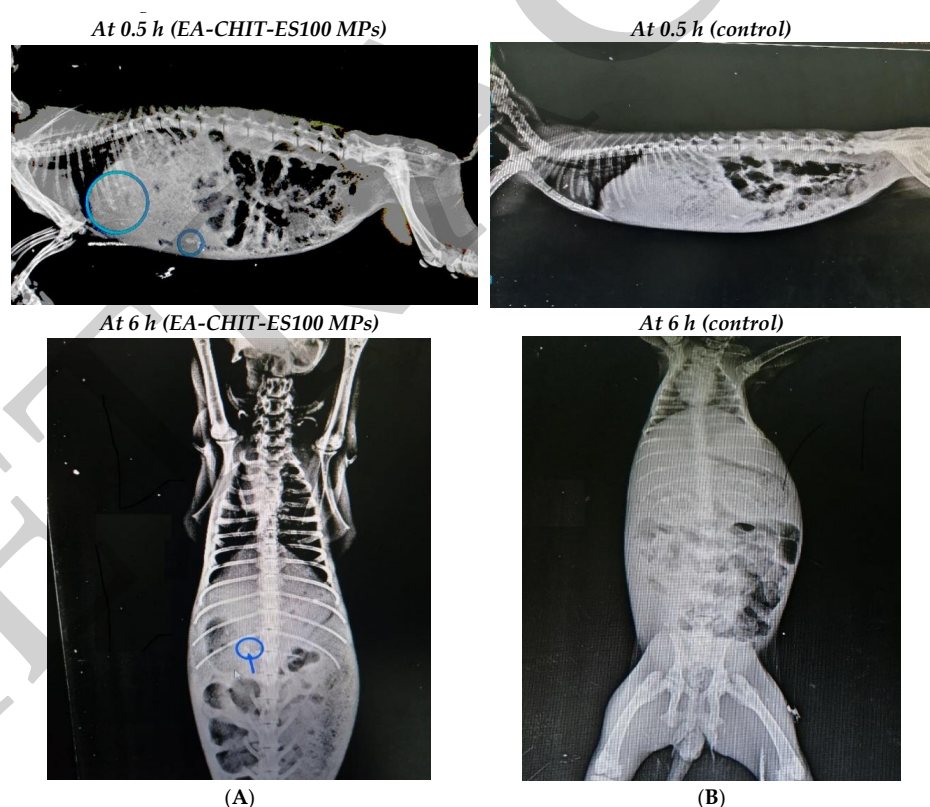

Figure 7. X-ray photographs of (**A**) EA-CHIT-ES100 MPs and (**B**) after 0.5 and 6 h.

4. Discussion

Glutaraldehyde cross-linking has been developed for stable EA MPs with spherical shape and size of approximately 200 ± 40 μm. The amino (CHIT)/glutaraldehyde molar ratio was (1:1). Previous reports indicated that both carbonyl groups of glutaraldehyde are involved in CHIT (amino group)

cross-linking [45]. The drug ionic interaction and hydrogen bonding among CHIT, glutaraldehyde, and EA can be explained by the high EE percentage of EA. An explanation of the in vitro EA release pattern may be given as such: only less than 8% of EA was released from 0 to 4 h, which is rationalized by ES100 (MPs coat) not dissolving in acidic pH (pKa 6). While EA release began to improve after 6 h (pH7.4), as ES100 dissolves at alkaline pH as a result of carboxylic groups ionization, which allows EA-CHIT particles to dissolve and release EA content [41]. The degradation of EA-CHIT MPs (uncoated MPs) could possibly be due to a hydrolytic reaction, whereby glucosamine–glucosamine, glucosamine–*N*-acetyl glucosamine, and *N*-acetyl glucosamine–*N*-acetyl glucosamine links are broken, causing increased release. CHIT degradation is dependent on variations in the distribution of acetamide groups in the chitosan molecule [46]. However, previous reports indicated that CHIT nano/microparticles crosslinked with glutaraldehyde are not degradable in a lysozyme solution [47]. Further, in a review about degradability of chitosan micro/nanoparticles, the authors stated: "To date, no complete in vitro degradation studies of chitosan micro/nanoparticles have been reported, and no degradation data are available in the biological system" [45].

EA formulated in CHIT and eurdragit S100 exhibited significantly enhanced cytotoxicity, as indicated by IC50 values, against colon cancer cells. This can be understood on the basis of the ability of CHIT to pass cellular membranes and enhance delivery of enclosed molecules [29,48,49]. However, the enhanced cytotoxicity of EA formulations in HCT 116 cells compared with EA.hy926 cells is not completely understood. The observed cytotoxicity of EA is consistent with previous reports indicating that its activity against HCT 116 cells is associated with Bax translocation to the mitochondria and reduction of PCNA expression [16]. In addition, CHIT's in vivo and in vitro activity against cancer cells has been investigated [16,50]. CHIT was shown to inhibit proliferation of human colorectal cells via inhibiting ornithine decarboxylases and, consequently, synthesis of polyamines required for DNA stabilization and cell replication. The effects of ornithine decarboxylases are inhibited by COS in human colorectal cells. These enzymes generate polyamines that stabilize newly formed DNA required for cancer cell proliferation [51,52].

This observed antiproliferative activity of the formulated EA double-coated with CHIT and ES100 was confirmed by assessing cell-cycle phases. The formula resulted in cells accumulating in the G2-M phase and increased pre-G1 fraction. These observations gain support by a previous study that indicated the ability of EA to accumulate HCT 15 colon adenocarcinoma cells in the G2-M phase and increase dead cells in the pre-G1 phase [10]. Also, another study revealed that CHIT coating enhanced curcumin-induced accumulation of HCT 116 cells in the G2-M phase [25]. The enhancement of dead cells in pre-G1 fractions strongly suggests that the prepared EA double-coating formula exhibits pro-apoptotic activity. This is consistent with the reported ability of EA to modify Gene Ontology (GO) and Kyoto Encyclopedia of Genes and Genomes (KEGG) pathways in HCT 116 cells and cause apoptosis and inhibition of proliferation [10].

Annexin V staining further substantiated the enhanced pro-apoptotic activity of EA-CHIT-ES100 MPs formula. The prepared EA formula was superior to pure EA in enhancing early and late apoptosis and total cell death. These results are supported by the ability of CHIT-ES100 coating to augment simvastatin apoptotic activity as indicated by annexin V staining of HCT 116 cells [36]. Additional support is offered by a study reporting the apoptotic efficiency of modified CHIT in human colon carcinoma HCT 116 cells [10]. In line with these data, caspase 3 content was significantly enhanced by challenging HCT 116 cells with the prepared EA CHIT-loaded ES100. Basically, EA has shown potent antiproliferative activities in different cancer cells lines, including colon cancer cells via enhancing caspases 9, 3, and 7 mRNA expression. Further, CHIT has been known to induce apoptosis via activation of caspase 3 in bladder [15], cervical [50], and colorectal [36] tumor cells. Also, the plain CHIT-ES100 coat significantly enhanced caspase 3 activity in colon cancer Caco-2 cells [15,53]. Thus, the observed augmented effects can be explained based on the collective actions of the individual ingredients used in the optimized formula.

Finally, colon targeting efficiency of the prepared CHIT-ES100 coat was evaluated via real-time X-ray radiography using an iohexol contrast medium in rabbits. Compared with iohexol (raw) filled hard gelatin capsules, the prepared formula delivered its content into the colon at 6–9 h, which is typically the time required for GIT contents to reach the colon [53]. The use of ES100 to target colonic tissues is well-acknowledged [25,30,41]. For instance, it has been used for colonic delivery of prednisolone [37]. In addition, our observations that EA release peaked at a pH of 7.4 in 6–9 h lend support to the radiographic data. In conclusion, EA-loaded CHIT coated with ES100 formula exhibited boosted cytotoxicity and proapoptotic activity against HCT 116 colon cancer cells as well as enhanced colon targeting potency.

References

1. Gou, M.; Men, K.; Shi, H.; Xiang, M.; Zhang, J.; Song, J.; Long, J.; Wan, Y.; Luo, F.; Zhao, X.; et al. Curcumin-loaded biodegradable polymeric micelles for colon cancer therapy in vitro and in vivo. *Nanoscale* **2011**, *3*, 1558–1567. [CrossRef] [PubMed]

2. Shirin, H.; Reddy, B.S.; Holt, P.R.; Agarwal, B.; Rao, C.V.; Bhendwal, S.; Ramey, W.R.; Shirin, H.; Reddy, B.S.; Holt, P.R. Lovastatin Augments Sulindac-Induced Apoptosis in Colon Cancer Cells and Potentiates Chemopreventive Effects of Sulindac. *Gastroenterology* **1999**, *117*, 838–847.

3. Xiao, B.; Merlin, D. Oral colon-specific therapeutic approaches toward treatment of inflammatory bowel disease. *Expert Opin. Drug Deliv.* **2012**, *9*, 1393–1407. [CrossRef] [PubMed]

4. Haggar, F.A.; Boushey, R.P. Colorectal cancer epidemiology: Incidence, mortality, survival, and risk factors. *Clin. Colon Rectal Surg.* **2009**, *22*, 191–197. [CrossRef] [PubMed]

5. World Health Organization. Cancer. Available online: https://www.who.int/health-topics/cancer#tab=overview (accessed on 6 September 2019).

6. Arnold, M.; Sierra, M.S.; Laversanne, M.; Soerjomataram, I.; Jemal, A.; Bray, F. Global patterns and trends in colorectal cancer incidence and mortality. *Gut* **2017**, *66*, 683–691. [CrossRef] [PubMed]

7. Zhang, H.; Jia, R.; Wang, C.; Hu, T.; Wang, F. Piceatannol promotes apoptosis via up-regulation of microRNA-129 expression in colorectal cancer cell lines. *Biochem. Biophys. Res. Commun.* **2014**, *452*, 775–781. [CrossRef]

8. Ryerson, A.B.; Eheman, C.R.; Altekruse, S.F.; Ward, J.W.; Jemal, A.; Sherman, R.L.; Henley, S.J.; Holtzman, D.; Lake, A.; Noone, A.M.; et al. Annual Report to the Nation on the Status of Cancer, 1975-2012, featuring the increasing incidence of liver cancer. *Cancer* **2016**, *122*, 1312–1337. [CrossRef]

9. Wolpin, B.M.; Mayer, R.J. Systemic Treatment of Colorectal Cancer. *Gastroenterology* **2008**, *134*, 1296. [CrossRef]

10. Umesalma, S.; Nagendraprabhu, P.; Sudhandiran, G. Ellagic acid inhibits proliferation and induced apoptosis via the Akt signaling pathway in HCT-15 colon adenocarcinoma cells. *Mol. Cell. Biochem.* **2015**, *399*, 303–313. [CrossRef]

11. Boukharta, M.; Jalbert, G.; Castonguay, A. Biodistribution of Ellagic Acid and Dose-Related Inhibition of Lung Tumorigenesis in A/J Mice. *Nutr. Cancer* **1992**, *18*, 181–189. [CrossRef]

12. Ceci, C.; Tentori, L.; Atzori, M.G.; Lacal, P.M.; Bonanno, E.; Scimeca, M.; Cicconi, R.; Mattei, M.; De Martino, M.G.; Vespasiani, G.; et al. Ellagic acid inhibits bladder cancer invasiveness and in vivo tumor growth. *Nutrients* **2016**, *8*, 744. [CrossRef]

13. Chen, H.S.; Bai, M.H.; Zhang, T.; Li, G.D.; Liu, M. Ellagic acid induces cell cycle arrest and apoptosis through TGF-β/Smad3 signaling pathway in human breast cancer MCF-7 cells. *Int. J. Oncol.* **2015**, *46*, 1730–1738. [CrossRef] [PubMed]

14. Ahire, V.; Kumar, A.; Mishra, K.P.; Kulkarni, G. Ellagic Acid Enhances Apoptotic Sensitivity of Breast Cancer Cells to γ-Radiation. *Nutr. Cancer* **2017**, *69*, 904–910. [CrossRef]

15. Ramadan, D.T.; Ali, M.A.M.; Yahya, S.M.; El-Sayed, W.M. Correlation between Antioxidant/Antimutagenic and Antiproliferative Activity of Some Phytochemicals. *Anticancer. Agents Med. Chem.* **2019**, *19*, 1481–1490. [CrossRef] [PubMed]

16. Yousef, A.I.; El-Masry, O.S.; Yassin, E.H. The anti-oncogenic influence of ellagic acid on colon cancer cells in leptin-enriched microenvironment. *Tumor Biol.* **2016**, *37*, 13345–13353. [CrossRef] [PubMed]

17. Fahmy, U.A. Augmentation of Fluvastatin Cytotoxicity Against Prostate Carcinoma PC3 Cell Line Utilizing Alpha Lipoic–Ellagic Acid Nanostructured Lipid Carrier Formula. *AAPS Pharmscitech* **2018**, *19*, 3454–3461. [CrossRef]

18. Zhang, H.M.; Zhao, L.; Li, H.; Xu, H.; Chen, W.W.; Tao, L. Research progress on the anticarcinogenic actions and mechanisms of ellagic acid. *Cancer Biol. Med.* **2014**, *11*, 92–100. [PubMed]

19. Mady, F.M.; Shaker, M.A. Enhanced anticancer activity and oral bioavailability of ellagic acid through encapsulation in biodegradable polymeric nanoparticles. *Int. J. Nanomed.* **2017**, *12*, 7405–7417. [CrossRef]

20. Cerdá, B.; Llorach, R.; Cerón, J.J.; Espín, J.C.; Tomás-Barberán, F.A. Evaluation of the bioavailability and metabolism in the rat of punicalagin, an antioxidant polyphenol from pomegranate juice. *Eur. J. Nutr.* **2003**, *42*, 18–28. [CrossRef]

21. Lei, F.; Xing, D.M.; Xiang, L.; Zhao, Y.N.; Wang, W.; Zhang, L.J.; Du, L.J. Pharmacokinetic study of ellagic acid in rat after oral administration of pomegranate leaf extract. *J. Chromatogr. B Anal. Technol. Biomed. Life Sci.* **2003**, *796*, 189–194. [CrossRef]

22. Seeram, N.P.; Lee, R.; Heber, D. Bioavailability of ellagic acid in human plasma after consumption of ellagitannins from pomegranate (*Punica granatum* L.) juice. *Clin. Chim. Acta* **2004**, *348*, 63–68. [CrossRef] [PubMed]

23. Whitley, A.C.; Stoner, G.D.; Darby, M.V.; Walle, T. Intestinal epithelial cell accumulation of the cancer preventive polyphenol ellagic acid—Extensive binding to protein and DNA. *Biochem. Pharm.* **2003**, *66*, 907–915. [CrossRef]

24. Aljaeid, B.M.; El-Say, K.M.; Hosny, K.M. Chitosan-TPP nanoparticles stabilized by poloxamer for controlling the release and enhancing the bioavailability of doxazosin mesylate: In Vitro, and in vivo evaluation. *Drug Dev. Ind. Pharm.* **2019**, *45*, 1130–1139. [CrossRef]

25. Khatik, R.; Mishra, R.; Verma, A.; Dwivedi, P.; Kumar, V.; Gupta, V.; Paliwal, S.K.; Mishra, P.R.; Dwivedi, A.K. Colon-specific delivery of curcumin by exploiting Eudragit-decorated chitosan nanoparticles in vitro and in vivo. *J. Nanoparticle Res.* **2013**, *15*. [CrossRef]

26. Ali, A.; Ahmed, S. A review on chitosan and its nanocomposites in drug delivery. *Int. J. Biol. Macromol.* **2018**, *109*, 273–286. [CrossRef] [PubMed]

27. Kurakula, M.; El-Helw, A.M.; Sobahi, T.R.; Abdelaal, M.Y. Chitosan based atorvastatin nanocrystals: Effect of cationic charge on particle size, formulation stability, and in-vivo efficacy. *Int. J. Nanomed.* **2015**, *10*, 321–334. [CrossRef] [PubMed]

28. Kozakevych, R.B.; Bolbukh, Y.M.; Tertykh, V.A. Controlled Release of Diclofenac Sodium from Silica-Chitosan Composites. *World J. Nano Sci. Eng.* **2013**, *03*, 69–78. [CrossRef]

29. Parveen, S.; Sahoo, S.K. Long circulating chitosan/PEG blended PLGA nanoparticle for tumor drug delivery. *Eur. J. Pharm.* **2011**, *670*, 372–383. [CrossRef]

30. Thakral, N.K.; Ray, A.R.; Majumdar, D.K. Eudragit S-100 entrapped chitosan microspheres of valdecoxib for colon cancer. *J. Mater. Sci. Mater. Med.* **2010**, *21*, 2691–2699. [CrossRef]

31. De Lima, I.A.; Khalil, N.M.; Tominaga, T.T.; Lechanteur, A.; Sarmento, B.; Mainardes, R.M. Mucoadhesive chitosan-coated PLGA nanoparticles for oral delivery of ferulic acid. *Artif. Cells Nanomed. Biotechnol.* **2018**, *46*, 993–1002. [CrossRef]

32. Marquié, C. Chemical reactions in cottonseed protein cross-linking by formaldehyde, glutaraldehyde, and glyoxal for the formation of protein films with enhanced mechanical properties. *J. Agric. Food Chem.* **2001**, *49*, 4676–4681. [CrossRef] [PubMed]

33. Niknejad, H.; Mahmoudzadeh, R. Comparison of different crosslinking methods for preparation of docetaxel-loaded albumin nanoparticles. *Iran. J. Pharm. Res.* **2015**, *14*, 385–394. [PubMed]

34. Zheng, B.L.; Liu, Q.Z.; Guo, C.S.; Wang, X.L.; He, L. Highly enantioselective direct aldol reaction catalyzed by cinchona derived primary amines. *Org. Biomol. Chem.* **2007**, *5*, 2913–2915. [CrossRef] [PubMed]

35. Kildeeva, N.R.; Perminov, P.A.; Vladimirov, L.V.; Novikov, V.V.; Mikhailov, S.N. About mechanism of chitosan cross-linking with glutaraldehyde. *Russ. J. Bioorganic Chem.* **2009**, *35*, 360–369. [CrossRef]

36. Alhakamy, N.A.; Fahmy, U.A.; Ahmed, O.A.A.; Caruso, G.; Caraci, F.; Asfour, H.Z.; Bakhrebah, M.A.; Alomary, M.N.; Abdulaal, W.H.; Okbazghi, S.Z.; et al. Chitosan coated microparticles enhance simvastatin colon targeting and pro-apoptotic activity. *Mar. Drugs* **2020**, *18*, 226. [CrossRef] [PubMed]

37. Onishi, H.; Kikuchi, H.; MacHida, Y. Comparison of simple Eudragit microparticles loaded with prednisolone and Eudragit-coated chitosan-succinyl-prednisolone conjugate microparticles: Part I. Particle characteristics and in vitro evaluation as a colonic delivery system. *Drug Dev. Ind. Pharm.* **2012**, *38*, 800–807. [CrossRef]

38. Boza, A.; Caraballo, I.; Alvarez-Fuentes, J.; Rabasco, A.M. Evaluation of Eudragit RS-PO and Ethocel 100 matrices for the controlled release of lobenzarit disodium. *Drug Dev. Ind. Pharm.* **1999**, *25*, 229–233. [CrossRef]

39. Yadav, S.K.; Mishra, S.; Mishra, B. Eudragit-based nanosuspension of poorly water-soluble drug: Formulation and in vitro-in vivo evaluation. *AAPS Pharmscitech* **2012**, *13*, 1031–1044. [CrossRef]

40. Rujivipat, S.; Bodmeier, R. Moisture plasticization for enteric Eudragit®L30D-55-coated pellets prior to compression into tablets. *Eur. J. Pharm. Biopharm.* **2012**, *81*, 223–229. [CrossRef]

41. Khan, M.Z.I.; Štedul, H.P.; Kurjaković, N. A pH-dependent colon-targeted oral drug delivery system using methacrylic acid copolymers. II. Manipulation of drug release using Eudragit®L100 and Eudragit S100 combinations. *Drug Dev. Ind. Pharm.* **2000**, *26*, 549–554. [CrossRef]

42. Vichai, V.; Kirtikara, K. Sulforhodamine B colorimetric assay for cytotoxicity screening. *Nat. Protoc.* **2006**, *1*, 1112–1116. [CrossRef] [PubMed]

43. Lee, J.J.; Kong, M.; Ayers, G.D.; Lotan, R. Interaction index and different methods for determining drug interaction in combination therapy. *J. Biopharm. Stat.* **2007**, *17*, 461–480. [CrossRef] [PubMed]

44. Van Engeland, M.; Nieland, L.J.W.; Ramaekers, F.C.S.; Schutte, B.; Reutelingsperger, C.P.M. Annexin V-affinity assay: A review on an apoptosis detection system based on phosphatidylserine exposure. *Cytometry* **1998**, *31*, 1–9. [CrossRef]

45. Islam, N.; Dmour, I.; Taha, M.O. Degradability of chitosan micro/nanoparticles for pulmonary drug delivery. *Heliyon* **2019**, *5*, e01684. [CrossRef] [PubMed]

46. Kofuji, K.; Qian, C.J.; Nishimura, M.; Sugiyama, I.; Murata, Y.; Kawashima, S. Relationship between physicochemical characteristics and functional properties of chitosan. *Eur. Polym. J.* **2005**, *41*, 2784–2791. [CrossRef]

47. Islam, N.; Wang, H.; Maqbool, F.; Ferro, V. In vitro enzymatic digestibility of glutaraldehyde-crosslinked chitosan nanoparticles in lysozyme solution and their applicability in pulmonary drug delivery. *Molecules* **2019**, *24*, 1271. [CrossRef]

48. Jiang, Y.; Yu, X.; Su, C.; Zhao, L.; Shi, Y. Chitosan nanoparticles induced the antitumor effect in hepatocellular carcinoma cells by regulating ROS-mediated mitochondrial damage and endoplasmic reticulum stress. *Artif. Cells Nanomed. Biotechnol.* **2019**, *47*, 747–756. [CrossRef]

49. Quagliariello, V.; Masarone, M.; Armenia, E.; Giudice, A.; Barbarisi, M.; Caraglia, M.; Barbarisi, A.; Persico, M. Chitosan-coated liposomes loaded with butyric acid demonstrate anticancer and anti-inflammatory activity in human hepatoma HepG2 cells. *Oncol. Rep.* **2018**, *41*, 1476–1486. [CrossRef]

50. Fadholly, A.; Ansori, A.N.M.; Proboningrat, A.; Nugraha, A.P.; Iskandar, R.P.D.; Rantam, F.A.; Sudjarwo, S.A. Apoptosis of hela cells via caspase-3 expression induced by chitosan-based nanoparticles of Annona squamosa leaf extract: In vitro study. *Indian J. Pharm. Educ. Res.* **2020**, *54*, 416–421. [CrossRef]

51. Shon, Y.H.; Nam, K.S. Chemopreventive effect of protein extract of Asterina pectinifera in HT-29 human colon adenocarcinoma cells. *Arch. Pharm. Res.* **2006**, *29*, 209–212. [CrossRef]

52. Shon, Y.H.; Nam, K.S. Inhibiton of polyamine biosynthesis in Acanthamoeba castellanii and 12-O-tetradecanoylphorbol-13-acetate-induced ornithine decarboxylase activity by chitosanoligosaccharide. *Biotechnol. Lett.* **2003**, *25*, 701–704. [CrossRef] [PubMed]

53. Jain, A.; Jain, R.; Jain, S.; Khatik, R.; Veer Kohli, D. Minicapsules encapsulating nanoparticles for targeting, apoptosis induction and treatment of colon cancer. *Artif. Cells Nanomed. Biotechnol.* **2019**, *47*, 1085–1093. [CrossRef] [PubMed]